Fracture process of a fiber bundle with strong disorder

J. Stat. Mech. (2016) 073211

(http://iopscience.iop.org/1742-5468/2016/7/073211)

Journal of Statistical Mechanics: Theory and Experiment
An IOP and SISSA journal

PAPER: Classical statistical mechanics, equilibrium and non-equilibrium

Fracture process of a fiber bundle with strong disorder

Zsuzsa Danku and Ferenc Kun

Department of Theoretical Physics, University of Debrecen, PO Box 5, H-4010 Debrecen, Hungary
E-mail: ferenc.kun@science.unideb.hu

Received 12 May 2016, revised 6 June 2016
Accepted for publication 11 June 2016
Published 28 July 2016

Online at stacks.iop.org/JSTAT/2016/073211
doi:10.1088/1742-5468/2016/07/073211

Abstract. We investigate the effect of the amount of disorder on the fracture process of heterogeneous materials in the framework of a fiber bundle model. The limit of high disorder is realized by introducing a power law distribution of fiber strength over an infinite range. We show that on decreasing the amount of disorder by controlling the exponent of the power law the system undergoes a transition from the quasi-brittle phase where fracture proceeds in bursts to the phase of perfectly brittle failure where the first fiber breaking triggers a catastrophic collapse. For equal load sharing in the quasi-brittle phase the fat tailed disorder distribution gives rise to a homogeneous fracture process where the sequence of breaking bursts does not show any acceleration as the load increases quasi-statically. The size of bursts is power law distributed with an exponent smaller than the usual mean field exponent of fiber bundles. We demonstrate by means of analytical and numerical calculations that the quasi-brittle to brittle transition is analogous to continuous phase transitions and determine the corresponding critical exponents. When the load sharing is localized to nearest neighbor intact fibers the overall characteristics of the failure process prove to be the same, however, with different critical exponents. We show that in the limit of the highest disorder considered the spatial structure of damage is identical with site percolation—however, approaching the critical point of perfect brittleness spatial correlations play an increasing role, which results in a different cluster structure of failed elements.

Keywords: avalanches, fracture, classical phase transitions

Contents

1. Introduction

Natural materials and most of the artificially made ones have an inherent disorder which appears at different length scales in the form of dislocations, flaws, microcracks, grain boundaries, or internal frictional interfaces [1]. When subject to mechanical load, this quenched structural disorder plays a decisive role in the emerging fracture process: disorder gives rise to strength reduction by introducing week locations where cracking can be initiated. For a fixed sample size the tensile strength is a stochastic variable described by a probability distribution [1–3]. Increasing the extension of samples a size effect emerges, i.e. the ultimate strength of disordered materials is a decreasing function of their size, which has to be taken into account in engineering design [3, 4]. The main benefit of disorder is that it stabilizes the fracture process, making it possible to arrest propagating cracks. As a consequence the fracture process of disordered materials is composed of a large number of crack nucleation—propagation—arrest steps which generate a sequence of precursory cracking avalanches. This crackling noise is of ultimate importance to work out forecasting technologies for natural catastrophes such as landslides and earthquakes, and for the catastrophic failure of engineering constructions [5, 6]. The degree of disorder present in materials affects fracture processes both on the macro- and micro-scales; however, detailed understanding of the relevant mechanisms is still lacking.

It is rather difficult to perform laboratory experiments precisely tuning the amount of a material's disorder. The length scale of disorder was controlled by heat treatment in phase-separated glasses [7] which proved to have an effect on the roughness of the generated crack surface. Sub-critical crack propagation was investigated in a sheet of paper under a constant external load where the paper was softened by introducing holes in different geometries. It was found that the increasing disorder slows down the

J. Stat. Mech. (2016) 073211

propagation of the crack [8]. Recently, it has been shown for the compressive failure of porous materials that the amount of structural disorder is crucial for forecasting the global failure, i.e. the higher the disorder is the more intensive precursory activity is obtained, which improves the precision of forecasting [9].

In theoretical studies of the effect of quenched disorder on fracture, discrete models of materials are indispensable. In the framework of discrete models either randomness is introduced for the strength of cohesive elements or random dilution is applied on a regular lattice, where the amount of disorder is controlled by the width of the strength distribution [10–14] and by the degree of dilution [2, 15] respectively. In these investigations the fiber bundle model (FBM) is a very useful tool since it captures the relevant aspects of fracture processes but it is still simple enough to obtain analytical solutions and to design efficient simulation techniques [16, 17]. In the present paper we use fiber bundle modeling to investigate the limiting case of high disorder for the fracture process of heterogeneous materials. A power law distribution of fiber strength is considered over an infinite range where the exponent of the distribution controls the amount of disorder. We demonstrate that on varying the amount of disorder the system undergoes a transition from a quasi-brittle phase with precursory bursting activity to a perfectly brittle phase where the first fiber breaking triggers catastrophic failure. In the quasi-brittle phase the high disorder has interesting consequences both on the macro- and micro-scales: the ultimate strength of the bundle increases with the system size, which is controlled by extreme order statistics of fibers' strength. Under quasi-statically increasing load the cracking bursts of fibers form a stationary sequence without any acceleration and signature of the imminent global failure of the system. Burst sizes are power law distributed, however, with a significantly lower exponent than with moderate disorder. Simulations revealed that even if strong stress concentration is introduced in the system by locally redistributing the load after breaking events, the overall behavior of the fracture process remains the same and the spatial structure of damage closely resembles percolation.

2. Fiber bundle model with strong disorder

In the model we consider N parallel fibers with linearly elastic behavior described by the same Young's modulus $E = 1$. Disorder is introduced in the system such that the failure threshold of fibers σ_{th} is a random variable, which takes values in the interval $\sigma_{\text{th}}^{\min} \leqslant \sigma_{\text{th}} < +\infty$ according to the probability density function (PDF)

$$p(\sigma_{\text{th}}) = \mu \sigma_{\text{th}}^{-1-\mu}. \tag{1}$$

The lower bound $\sigma_{\text{th}}^{\min}$ has a finite value $\sigma_{\text{th}}^{\min} = 1$ but the strength values σ_{th} cover an infinite range. A very important feature of $p(\sigma_{\text{th}})$ is that the amount of disorder can be controlled by varying the exponent μ in such a way that increasing μ results in a lower disorder. In our study we focus on the parameter range $0 < \mu \leqslant 1$, where the disorder is so high that even the first moment of the distribution (1) does not exist; however, normalizability is ensured (see figure 1(*a*) for illustration). As a first step, we assume that under an increasing external load σ when a fiber breaks its load is

J. Stat. Mech. (2016) 073211

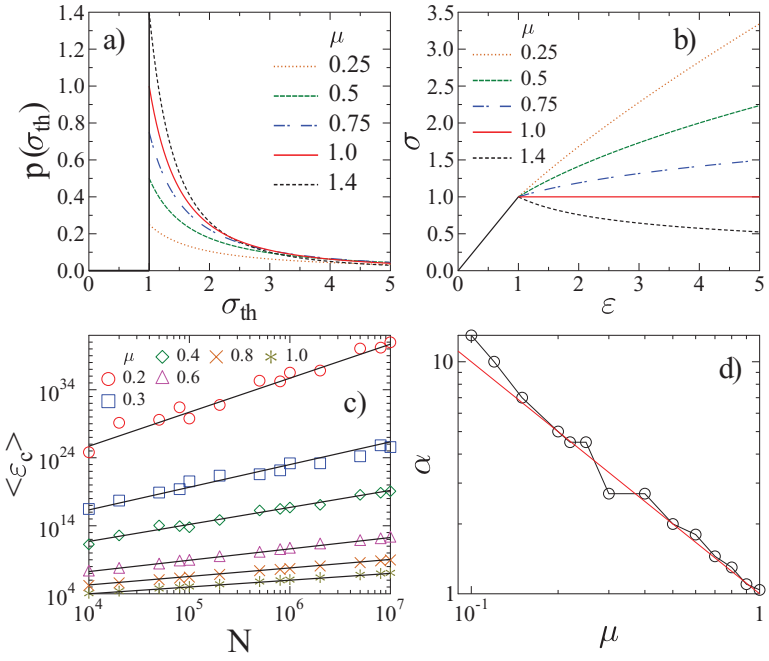

Figure 1. (*a*) Probability density of failure thresholds for several values of the control parameter μ. (*b*) Constitutive curve $\sigma(\varepsilon)$ of the system for several different values of the exponent μ. In the parameter range $\mu < 1$ the constitutive curve monotonically increases, while for $\mu > 1$ it has a sharp maximum at $\sigma_{\rm th}^{\rm min} = 1$. (*c*) Average critical strain $\langle \varepsilon_{\rm c} \rangle$ of the bundle where global failure occurs as a function of the system size N for several values of the exponent μ. The straight lines represent power law fits. (*d*) Exponent of the size dependence of the critical strain $\langle \varepsilon_{\rm c} \rangle$. The straight line represents the power law for exponent -1.

equally redistributed over all intact fibers. In this equal load sharing (ELS) limit the constitutive equation $\sigma(\varepsilon)$ of the model can be obtained from the generic expression $\sigma(\varepsilon) = E\varepsilon\,[1 - P(E\varepsilon)]$ where P denotes the cumulative distribution function (CDF) of failure thresholds, and the term $1 - P(E\varepsilon)$ is the fraction of fibers that are intact at the deformation ε. For our model the constitutive equation $\sigma(\varepsilon)$ can be cast in the form

$$\sigma(\varepsilon) = \begin{cases} E\varepsilon & \text{for} \quad \varepsilon \leqslant \varepsilon_0, \\ E\varepsilon^{1-\mu} & \text{for} \quad \varepsilon > \varepsilon_0, \end{cases} \tag{2}$$

where the threshold strain ε_0 has the value $\varepsilon_0 = \sigma_{\rm th}^{\rm min}/E = 1$. Figure 1(*b*) shows that below ε_0 linearly elastic behavior is obtained since no fibers can break. As breaking sets on for $\varepsilon > \varepsilon_0$, non-linearity of $\sigma(\varepsilon)$ emerges, which gets stronger with increasing μ. It can be seen that on varying μ as a control parameter the constitutive behavior of the system has two qualitatively different regimes: for $\mu < 1$ the non-linear increase of $\sigma(\varepsilon)$ implies a quasi-brittle response of the system where under stress controlled loading the fracture of the bundle would proceed by stable damaging as fibers gradually break. However, increasing μ above 1 the constitutive curve becomes decreasing beyond the threshold strain ε_0, having a sharp maximum at ε_0. This functional form implies that all fibers break immediately in a catastrophic avalanche as the external load surpasses the value $E\varepsilon_0$. Since linear response is followed by sudden collapse the behavior of the

J. Stat. Mech. (2016) 073211

system is perfectly brittle in the parameter range $\mu > 1$. The transition from the quasi-brittle to the brittle phase occurs at the critical point $\mu_c = 1$ where the stress σ becomes constant $\sigma = E\varepsilon_0$, independent of the strain ε (see figure 1(*b*)).

3. Fracture strength

An interesting feature of the constitutive equation (2) is that in the quasi-brittle phase it does not have a local maximum so that it is monotonically increasing until the last fiber breaks. This has the consequence that even under stress controlled loading no catastrophic avalanche of breaking emerges so that in a finite bundle of N fibers the fracture strength σ_c and the corresponding fracture strain ε_c are determined by the breaking threshold of the strongest fiber. Hence, the macroscopic strength of the system is controlled by the extreme order statistics of fibers' strength [18, 19]. The average failure strain $\langle\varepsilon_c\rangle$ of the bundle can simply be obtained as the average value of the largest threshold strain ε_{th}^{max} of fibers, where the relation $\sigma_{th} = E\varepsilon_{th}$ holds for the stress and strain thresholds of single fibers. According to the generic result of extreme order statistics [18, 19] the average $\langle\varepsilon_{th}^{max}\rangle_N$ of the largest of N independent identically distributed random variables can be determined as

$$\langle\varepsilon_c\rangle = \langle\varepsilon_{th}^{max}\rangle_N = P^{-1}\left(1 - \frac{1}{N+1}\right), \tag{3}$$

where P^{-1} denotes the inverse of the cumulative distribution function P. Substituting the distribution function P of our model the above equation yields

$$\langle\varepsilon_c\rangle = \left(\frac{1}{N+1}\right)^{-1/\mu} \approx N^{1/\mu}. \tag{4}$$

The result shows that the strength of the bundle increases as a power law of the system size N, which is in a strong contrast with the usual decreasing strength of the disorder dominated size effect of heterogeneous materials. In the simulations $\langle\varepsilon_c\rangle$ was determined by directly averaging the strain at which the last avalanche occurred. Figure 1(*c*) demonstrates that the numerical results are consistent with the theoretical expectations and can be very well fitted by the power law $\langle\varepsilon_c\rangle \sim N^{\alpha}$, where the exponent α has an excellent agreement with the analytical prediction $\alpha = 1/\mu$ (see figure 1(*d*)).

4. Crackling noise

The quasi-static loading of the sample is carried out by increasing the external load to provoke the breaking of a single fiber. The failure event is followed by the redistribution of load where each intact fiber receives the same load increment under ELS conditions. The elevated load may give rise to additional breakings, and in turn the repeated steps of load redistribution and breaking can generate a failure avalanche. The size Δ of the avalanche can be characterized by the number of fibers breaking in the correlated

J. Stat. Mech. (2016) 073211

trail. The microscopic origin of the perfectly brittle behavior for $\mu > 1$ is that the first breaking event, i.e. the breaking of the weakest fiber immediately triggers an avalanche that cannot stop leading to catastrophic collapse. However, in the quasi-brittle phase the fracture of the bundle proceeds in a sequence of bursts with size Δ spanning a broad range. It can be observed in figure 2(*a*) for a single sample that the sequence of breaking bursts has an astonishing stationarity, i.e. in spite of the increasing load the moving average of event sizes and their fluctuations remain practically constant. Note that the absence of a catastrophic avalanche means that even the last avalanche obeys the same statistics as all others. This behavior is in strong contrast to what is usually observed when the disorder is moderate: as the load increases the size of bursts spans a broader and broader range when approaching global failure so that the average event size rapidly increases towards failure [16, 20, 21].

The statistics of crackling avalanches is characterized by the distribution of their size $p(\Delta)$, which is presented in figure 2(*b*) for several values of the exponent μ. Power law behavior is evidenced, which is followed by an exponential cutoff. It can be observed in the figure that as μ approaches 1 the cutoff burst size increases and finally diverges so that for $\mu = 1$ the complete distribution can be described by a single power law. The most remarkable feature of the results is that the exponent ξ of the power law regime is $\xi = 3/2$—significantly lower than the usual mean field exponent $\xi = 5/2$ of fiber bundles found for a broad class of disorder distributions. The lower value of the exponent implies a higher fraction of larger avalanches during the breaking process of the highly disordered system.

In order to understand the absence of acceleration in the avalanche activity and the emergence of the low exponent of the size distribution it is instructive to calculate the average number a of fiber breakings triggered immediately by the failure of a single fiber at the strain ε [20, 21]. Since the load $\sigma = E\varepsilon$ dropped by the broken fiber is equally shared by all the intact fibers of number $N[1 - P(\sigma)]$ the stress increment $\Delta\sigma$ they experience is $\Delta\sigma = \sigma/N[1 - P(\sigma)]$. Eventually, a follows by multiplying $\Delta\sigma$ with the probability density $p(E\varepsilon)$ of failure thresholds and with the total number of fibers N

$$a(\varepsilon) = \frac{E\varepsilon p(E\varepsilon)}{1 - P(E\varepsilon)} = \mu. \tag{5}$$

The right-hand side of the equation was obtained by substituting the PDF p and the CDF P of failure thresholds of our model. It follows that in our FBM the probability of triggering avalanches does not depend on where the system is during the loading process, and hence, from the viewpoint of avalanches all points of the constitutive curve are equivalent to each other. This mechanism explains the absence of increasing bursting activity in figure 2 with increasing load. Note that a catastrophic avalanche occurs when $a(\sigma) > 1$ [20], which can only be obtained in our case for $\mu > 1$. Hence, for any $\mu < 1$ the system approaches failure in a stable way, all fibers breaking in finite avalanches.

The complete size distribution $p(\Delta)$ can be obtained analytically by substituting $a(\varepsilon)$ into the generic form [20–22]

$$\frac{p(\Delta)}{N} = \frac{\Delta^{\Delta-1}\mathrm{e}^{-\Delta}}{\Delta!} \int_0^{x_c} p(x)a(x)[1 - a(x)]^{\Delta-1}\mathrm{e}^{\Delta a(x)}\mathrm{d}x \tag{6}$$

J. Stat. Mech. (2016) 073211

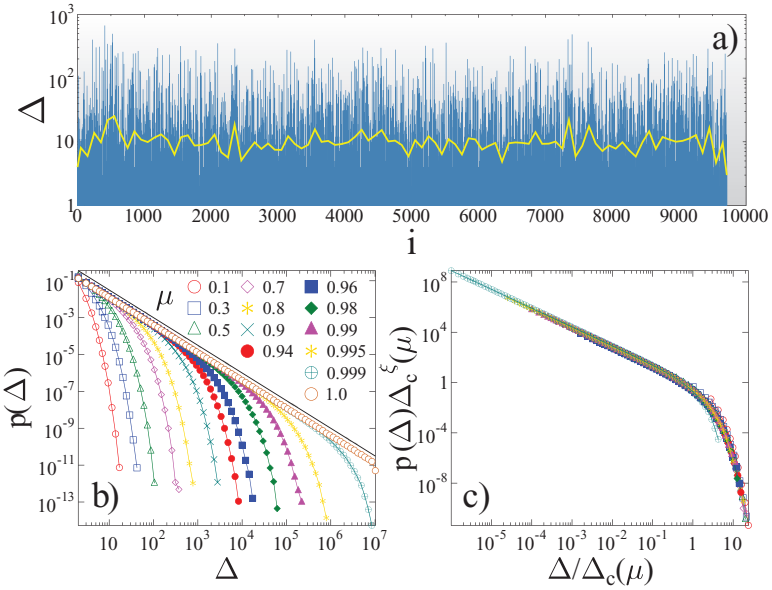

Figure 2. (*a*) Sequence of bursts emerging during the quasi-static loading of a bundle of $N = 10^5$ fibers with $\mu = 0.9$. The burst size Δ is plotted as a function of the order number i of the crackling event. The bold yellow line represents the moving average of the event size considering 100 consecutive bursts. No acceleration towards global failure can be pointed out. (*b*) Size distribution of avalanches $p(\Delta)$ for several values of the exponent μ. Power law functional form is obtained, followed by an exponential cutoff. The straight line represents a power law with exponent 3/2. (*c*) Data collapse analysis of the avalanche size distributions. The data presented in (*b*) is replotted such that the two axes are rescaled with powers of the characteristic burst size $\Delta_c(\mu)$.

where for the upper limit of integration x_c we have to insert the strength of the bundle. Inserting our PDF and the expression (5) of the average number of triggered failures a, and utilizing the approximation $\Delta! \simeq \Delta^{\Delta} e^{-\Delta}\sqrt{2\pi\Delta}$ the analytic result can be cast into the final form

$$\frac{p(\Delta)}{N} \simeq \Delta^{-3/2} e^{-\Delta/\Delta_c}. \tag{7}$$

A power law of exponent $\xi = 3/2$ is obtained followed by an exponential cutoff, in agreement with the numerical results. Here, Δ_c denotes the characteristic burst size which controls the cutoff of the distribution. The value of Δ_c depends solely on the control parameter

$$\Delta_c = \frac{1}{\mu - 1 - \ln \mu}. \tag{8}$$

To demonstrate the consistency of the results in figure 2(*c*) we present the scaling plot of the avalanche size distributions where the two axes of figure 2(*b*) are rescaled with powers of Δ_c, using $\kappa = 1$ and $\kappa\xi = 3/2$ for the exponents on the horizontal and vertical axes respectively. The high quality data collapse underlines that the analytical solution provides a comprehensive description of the avalanche activity of the model.

J. Stat. Mech. (2016) 073211

It has been shown in equal load sharing FBMs that the probability distribution of the size of bursts has a power law functional form where the exponent exhibits a high degree of universality with respect to the form and amount of disorder: for disorder distributions, where the constitutive curve $\sigma(\varepsilon)$ of the system has a quadratic maximum, the burst size exponent is 5/2 [16]. Reducing the disorder by making the distribution of fibers' strength narrower, a crossover is obtained to a lower exponent 3/2 [13, 20, 23, 24]. The same happens when constraining the avalanche statistics to windows shrinking towards global failure—hence, the crossover has been suggested as an early signature of the imminent failure event [24]. An important consequence of our results is that at any point of the loading process avalanches of the same size range can pop up, and hence, the distribution does not evolve, both the exponent and the cutoff size remain the same wherever we measure them during the loading process.

5. Critical exponents

As the control parameter μ approaches the critical value μ_c from below the system undergoes a phase transition from quasi-brittle to perfectly brittle response. We used analytical calculations and finite size scaling of the simulated data to determine the critical exponents of the transition. Based on the Taylor expansion $\ln(1+x) \approx x - x^2/2$ in (8) it can be shown that as μ approaches 1 the cutoff burst size has a power law divergence as a function of the distance from the critical value $\mu_c = 1$

$$\Delta_c \sim (\mu_c - \mu)^{-1/\sigma_\Delta}, \tag{9}$$

where the value of the cutoff exponent of avalanche sizes is $\sigma_\Delta = 1/2$.

Of course, in a finite system of N fibers deviations occur from the analytical solution of the infinite system size where even the critical point μ_c has size dependence. In order to obtain a detailed characterization of how the system approaches the critical point of perfectly brittle behavior with increasing μ, we determined the average burst size $\langle\Delta\rangle$ as a function of μ for several system sizes N. For $\langle\Delta\rangle$ first the average burst size of single samples is calculated as the second moment $M_2 = \sum_i \Delta_i^2$ of burst sizes divided by the first one $M_1 = \sum_i \Delta_i$, and then this quantity is averaged over a large number of samples. Note that the largest burst is always omitted in the summation. Figure 3(*a*) presents that for low μ values the average burst size falls close to one, indicating that nearly all fibers break one-by-one. When approaching the brittle phase larger and larger bursts can emerge and $\langle\Delta\rangle$ develops a sharp peak in the vicinity of $\mu_c = 1$. The finite values $\langle\Delta\rangle > 0$ observed for $\mu > 1$ are obtained due to the finite size effect on the critical point. Assuming that the quasi-brittle to brittle transition is analogous to continuous phase transitions power law divergence of $\langle\Delta\rangle$ can be expected

$$\langle\Delta\rangle \sim (\mu_c - \mu)^{-\gamma}, \tag{10}$$

which defines the γ exponent of the transition. Since the exponent ξ of the burst size distribution is less than 2, both the first M_1 and second M_2 moments of burst sizes diverge in an infinite system. This has the consequence that the average burst size is proportional to the cutoff size $\langle\Delta\rangle \sim \Delta_c$, which implies the relation $\gamma = 1/\sigma$ of the two

J. Stat. Mech. (2016) 073211

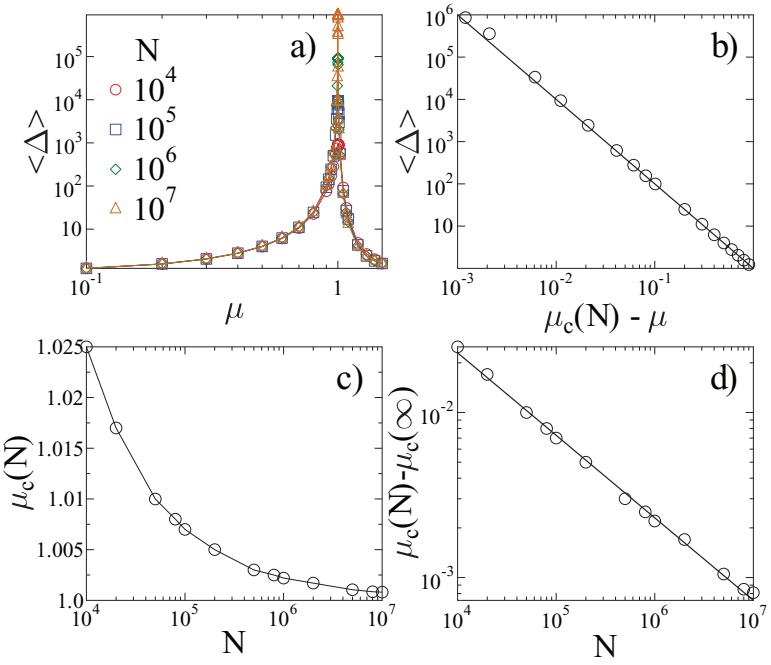

Figure 3. (*a*) Average size of bursts $\langle\Delta\rangle$ as a function of μ for system sizes covering three orders of magnitude. (*b*) The average burst size $\langle\Delta\rangle$ of $N = 10^7$ is replotted as a function of the distance from the critical point μ_c, where $\mu_c = 1.0009$ was used. The straight line represents a power law of exponent 2. (*c*) The critical point μ_c of finite size systems as a function of the number of fibers N. (*d*) The difference of the finite size critical point and that of the infinite system $\mu_c(N) - \mu_c(\infty)$ as a function of N. The straight line represents a power law of exponent 1/2.

critical exponents. In order to numerically verify the analytical predictions, we plotted the average burst size $\langle\Delta\rangle$ as a function of the distance from the critical point $\mu_c - \mu$, varying the value of μ_c until the best straight line is obtained on a double logarithmic plot. The procedure is illustrated in figure 3(*b*) for the system size $N = 10^7$. A high quality power law of exponent 2 is obtained in the figure with the finite size critical point $\mu_c(N = 10^7) = 1.0009(2)$ in an excellent agreement with the analytical considerations.

The value of the finite size critical point $\mu_c(N)$ is presented in figure 3(*c*) for system sizes N covering three orders of magnitude. It can be observed that $\mu_c(N)$ converges towards 1 with increasing N and obeys the scaling law

$$\mu_c(N) = \mu_c(\infty) + BN^{-1/\nu}, \tag{11}$$

characteristic for continuous phase transitions. Here $\mu_c(\infty) = 1$ denotes the critical point of the infinite system, and ν is the correlation length exponent of the transition. It can be seen in figure 3(*d*) that the difference $\mu_c(N) - \mu_c(\infty)$ decreases as a power law of N with an exponent 1/2, which implies $\nu = 2$ for our model.

When studying the phase transition nature of fracture phenomena the order parameter is typically defined in terms of the fraction of fibers which break up to the critical point of the loading process. However, for the quasi-brittle to brittle transition of highly disordered systems this fraction is always 1 and 0 in the quasi-brittle and brittle phases respectively, without any dependence on the distance from the critical point.

J. Stat. Mech. (2016) 073211

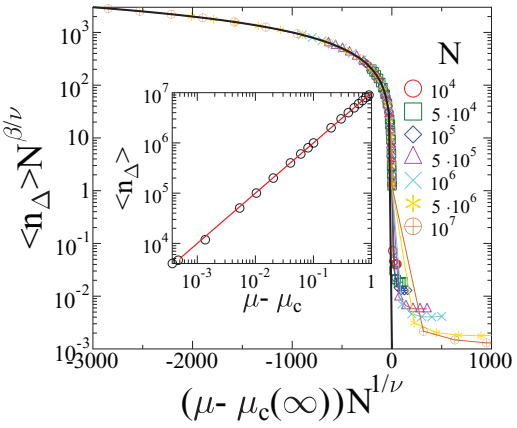

Figure 4. Scaling collapse of the order parameter of the transition. Rescaling the two axes according to (12) a high quality data collapse is obtained. Inset: the order parameter $\langle n_\Delta \rangle$ as a function of the distance from the critical point $\mu - \mu_c$ for the system of $N = 10^7$ fibers. The straight line represents a power law of exponent 1.

To characterize in which phase the system is when changing the control parameter μ, we define the order parameter of the transition $\langle n_\Delta \rangle$ as the average $\langle N_\Delta \rangle$ of the number of bursts N_Δ before global failure normalized by the total number of fibers N so that $\langle n_\Delta \rangle = \langle N_\Delta \rangle / N$. Since far below the critical point $\mu \ll \mu_c$ all avalanches are small (most of them have size 1) the control parameter has the value $\langle n_\Delta \rangle \approx 1$, while it tends to zero when approaching μ_c from below and it is zero in the brittle phase. For the continuous quasi-brittle to brittle transition power law functional form

$$\langle n_\Delta \rangle \sim (\mu_c - \mu)^\beta \tag{12}$$

is expected for $\mu < \mu_c$, which defines the order parameter exponent β of the transition. Figure 4 presents the scaling collapse of the order parameter obtained at different system sizes assuming the scaling structure

$$\langle n_\Delta \rangle(\mu, N) = N^{-\beta/\nu} \Psi((\mu - \mu_c(\infty))N^{1/\nu}), \tag{13}$$

where $\Psi(x)$ denotes the scaling function. Best collapse is obtained with the critical exponents $\beta = 1$ and $\nu = 2$.

6. Localized load sharing

In the case of equal load sharing studied so far, all fibers keep the same load. As the external load increases fibers gradually break but in spite of this the acceleration towards failure is completely missing. The qualitative explanation is that although the load bearing cross section of the bundle decreases and the load per fiber increases, the remaining fibers are always strong enough to ensure stability.

When the load sharing is localized (LLS) stress concentration develops around failed regions which in turn induces spatial correlation in the breaking process [13, 21, 22, 25, 26]. It has been shown in FBMs that as a consequence, for moderate disorder the system becomes more brittle and fails earlier at lower loads than in ELS [13, 26–28].

J. Stat. Mech. (2016) 073211

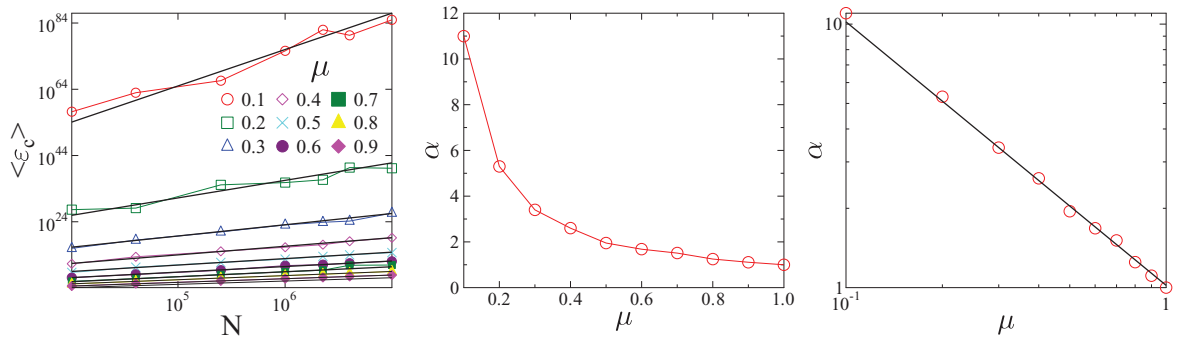

Figure 5. (a) Critical deformation $\langle \varepsilon_c \rangle$ of LLS bundles as a function of the system size N for several values of μ. Power law behavior is obtained. (b) The exponent α of the size dependence as a function of the control parameter μ. (c) The μ-dependence of α is described by a power law of exponent 1, similarly to the ELS case.

In order to see if this qualitative picture is valid when the disorder is high we carried out LLS simulations on a square lattice of size $L = 2001$, equally redistributing the load of broken fibers on their intact nearest neighbors in the lattice.

Figure 5 shows that for strong disorder the size dependence of the macroscopic strength of the LLS bundle has the same functional form as in the ELS case, i.e. $\langle \varepsilon_c \rangle$ increases as a power law of N (figure 5(a)) and the μ dependence of $\langle \varepsilon_c \rangle$ is also consistent with the analytic prediction of extreme order statistics (figures 5(b), (c)). The result shows that on the macro-level the spatial correlation introduced by the localized load sharing does not have any apparent consequence, even for the lowest disorder $\mu \to 1$ the macroscopic strength is controlled by the strongest fibers.

Figure 6 demonstrates that the burst size distributions $p(\Delta)$ have the same trend when the exponent μ of the disorder distribution approaches 1 as for the ELS counterpart: power law distributions are obtained with a diverging cutoff in the limit of $\mu \to 1$. It is interesting to note that the stress concentration around failed regions gives rise to a higher exponent $\xi = 1.8 \pm 0.05$ of $p(\Delta)$ which implies a somewhat lower frequency of large size bursts compared to the ELS. The high quality data collapse of the distributions of different μ values in figure 6(a) was obtained with the cutoff exponent $\sigma_\Delta = 0.3(3)$.

In order to perform scaling analysis in terms of system size N simulations were carried out on square lattices of size $L = 101$, 201, 501, 1001, 1501, 2001, 3151. The correlation length critical exponent $\nu = 2.5(5)$ was determined by analyzing the system size dependence of the critical point $\mu_c(N)$, which is highlighted in figure 6(b). The finite size scaling of the order parameter was used to obtain the β exponent $\beta = 0.8(3)$ of the quasi-brittle to brittle transition (see figure 6(c)). The average burst size $\langle \Delta \rangle$ was also found to have the same diverging behavior as in ELS described by the critical exponent $\gamma = 1.9(2)$ (not presented in figure).

The localized redistribution of load has the consequence that fibers breaking in a correlated avalanche form a connected cluster. In later stages of the failure process it may occur that intact fibers get isolated so that when they break the range of load redistribution is gradually extended until at least one intact fiber is found which then

J. Stat. Mech. (2016) 073211

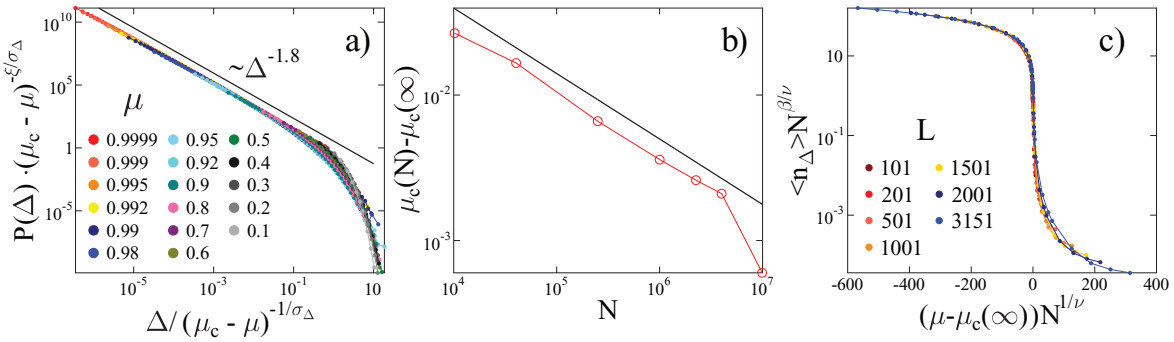

Figure 6. (*a*) Scaling collapse of the burst size distributions obtained at different μ values. (*b*) The critical point of finite systems $\mu_c(N)$ was determined based on the average bursts size. Using the scaling ansatz (11) the correlation length exponent ν could be obtained. (*c*) The order parameter obeys the same scaling form (13), which yields the β exponent.

gets the load. Intact fibers along the perimeter of clusters are highly stressed since they share the total load dropped by the fibers of the interior of the clusters. This damage structure has the consequence that for moderate disorder the clusters are space filling compact objects which remain small compared to the system size until failure. The final catastrophic avalanche is typically initiated by the breaking of a perimeter fiber. Figure 7 presents snapshots of the evolution of an LLS bundle of size $L = 2001$ for $\mu = 0.9$ where avalanches are highlighted by different colors. It can be observed that due to the high disorder the avalanches are not compact but they have a rather diffuse interior. At the beginning of the breaking process spreading avalanches do not affect each other; however, as the number of broken fibers N_b increases avalanches merge and form large broken clusters (cracks in the model). Large avalanches already occur at early stages of the fracture process; due to their diffuse structure in later stages small avalanches may nucleate even in the internal holes of the extended ones. The degree of damage in the bundle can be characterized by the fraction of broken fibers $n_b = N_b/N$, which increases from 0 to 1 as the loading proceeds. It is interesting to note that even at high values of n_b, where large clusters dominate the damage structure, the stability of the LLS system is retained, which is in strong contrast to the highly brittle behaviour of LLS bundles with moderate disorder [13, 26, 29].

In order to quantify the evolution of the cluster structure of broken fibers during the loading process, we determined the average value $\langle S \rangle$ of the size S of clusters as a function of n_b. $\langle S \rangle$ is defined as the ratio of the second and first moments $M_2 = \sum_i S_i^2$, $M_1 = \sum_i S_i$ of cluster sizes, where the largest cluster is omitted in the summation. The value of M_2/M_1 is averaged over 5000 simulations in bins of n_b. The results are presented in figure 8 for four values of the μ exponent. It can be observed that for all μ the $\langle S \rangle(n_b)$ curves have a sharp maximum, which indicates the emergence of a giant cluster at a critical damage fraction n_b^c. Since the failure process is dominated by the disorder of fibers' strength the cluster structure can be expected to be similar to the site percolation problem on a square lattice where n_b is analogous to the site occupation probability [30]. This is confirmed by the fact that when μ decreases, i.e. the amount of disorder increases, the critical point n_b^c gradually shifts to the site percolation critical point $n_b \approx 0.5923$ on a square lattice, while for higher values $\mu \to 1$ the giant cluster

J. Stat. Mech. (2016) 073211

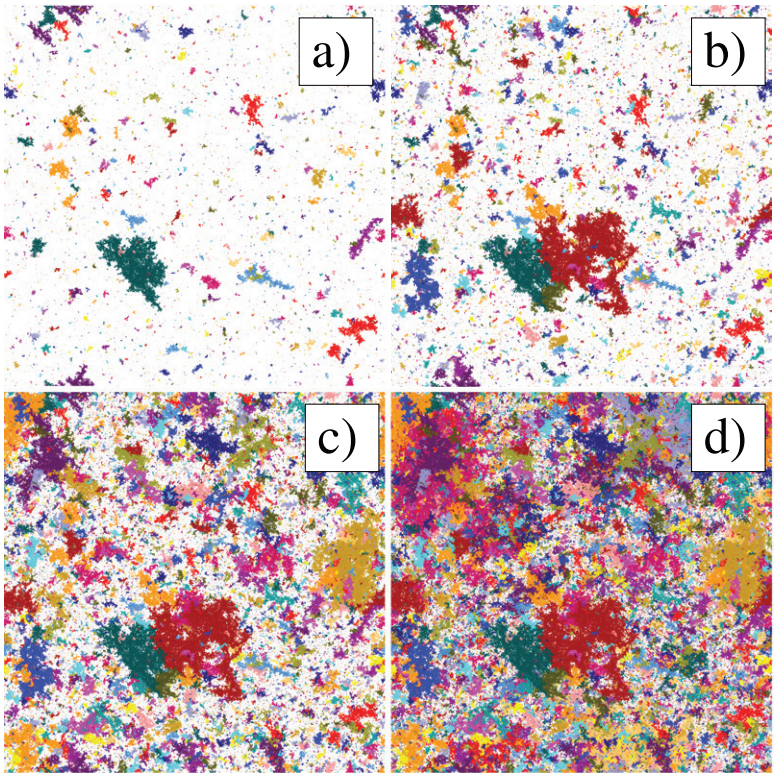

Figure 7. Snapshots of the evolving breaking process on a square lattice of size $L = 2001$ with $\mu = 0.9$ using periodic boundary conditions. Avalanches are highlighted by randomly assigned colors. At early stages of the fracture process ((*a*), (*b*)) bursts can evolve independently of each other; however, later on the merging of bursts dominates.

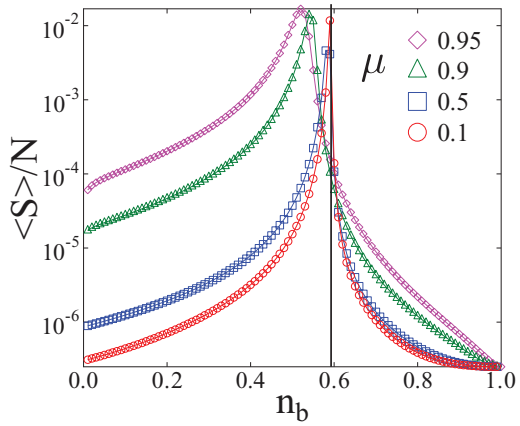

Figure 8. Average size of clusters $\langle S \rangle$ as a function of the fraction of broken fibers n_b. As μ decreases the position of the maximum n_b^c tends to critical occupation probability p_c of site percolation on a square lattice indicated by the vertical straight line.

emerges earlier. The reason is that for low μ exponents all avalanches are small so that in the limit of $\mu \to 0$ the disorder is so high that the fibers practically break one-by-one and the entire breaking process can be considered as a sequence of random nucleations,

J. Stat. Mech. (2016) 073211

as it is in percolation. At higher μ the lower disorder gives more room for the stress concentration, which in turn gives rise to extended avalanches and a stronger spacial correlation of local breakings. Since large avalanches can already be triggered at the beginning of the fracture process (see also figure 7), large clusters can appear even at low damage fractions, which makes the $\langle S\rangle(n_b)$ strongly asymmetric in figure 8 for high μ values.

A more detailed picture is provided by figure 9 which shows the size distribution of clusters $p(S)$ at several values of n_b both below and above the corresponding critical point n_b^c for two values of μ. Power law distributions are obtained, followed by an exponential cutoff

$$p(S) \sim S^{-\tau} \exp(-S/S_c), \tag{14}$$

where the cutoff cluster size S_c is controlled by the value of n_b. It can be observed that S_c tends to diverge as the critical damage fraction n_b^c is approached from both sides. Careful scaling analysis revealed that below and above the critical point n_b^c the exponent τ of the power law regime has different values. In figures 9((*b*), (*c*)) and ((*e*), (*f*)) we rescaled the avalanche size distributions with powers of the distance from the critical point $|n_b - n_b^c|$, tuning the scaling exponents along the horizontal and vertical axis until best collapse is achieved. The scaling functions can be well fitted with the exponents $\tau = 1.67$ and $\tau = 2.1$ ($\mu = 0.1$), and $\tau = 1.77$ and $\tau = 2.0$ ($\mu = 0.9$), respectively below and above the corresponding n_b^c (see figure 9). Clusters of broken fibers are generated by avalanches. At the beginning of the fracture process the merging of the clusters of individual avalanches is practically negligible—hence, below the critical damage fraction n_b^c the value of the exponent τ of the cluster size distribution $p(S)$ should be close to the exponent ξ of the avalanche size distribution $p(\Delta)$. Above n_b^c the merging of avalanches dominates, which gives rise to a steeper cluster size distribution with a τ greater than ξ. The values of τ determined numerically slightly depend on the control parameter μ falling in the range $\tau = 1.65$–1.95 below and $\tau = 1.95$–2.1 above n_b^c, which is consistent with the above arguments.

The good quality data collapse of $p(S)$ also implies that the cutoff cluster size S_c has a power law dependence on the distance from the critical point n_b^c

$$S_c \sim |n_b - n_b^c|^{-1/\sigma_S}. \tag{15}$$

The value of the cutoff exponent σ_S falls in the range 0.25–0.5, depending on the value of the control parameter μ.

7. Discussion

The presence of disorder makes the fracture process jerky where damage accumulates in intermittent avalanches that can be recorded in the form of crackling noise. Forecasting technologies of global failure of engineering construction or natural catastrophes like landslides, collapse of rockwalls, earthquakes, volcanic eruptions strongly rely on identifying signatures of the imminent failure based on the acceleration of crackling signals. In the present paper we showed in a fiber bundle model that this very important effect

J. Stat. Mech. (2016) 073211

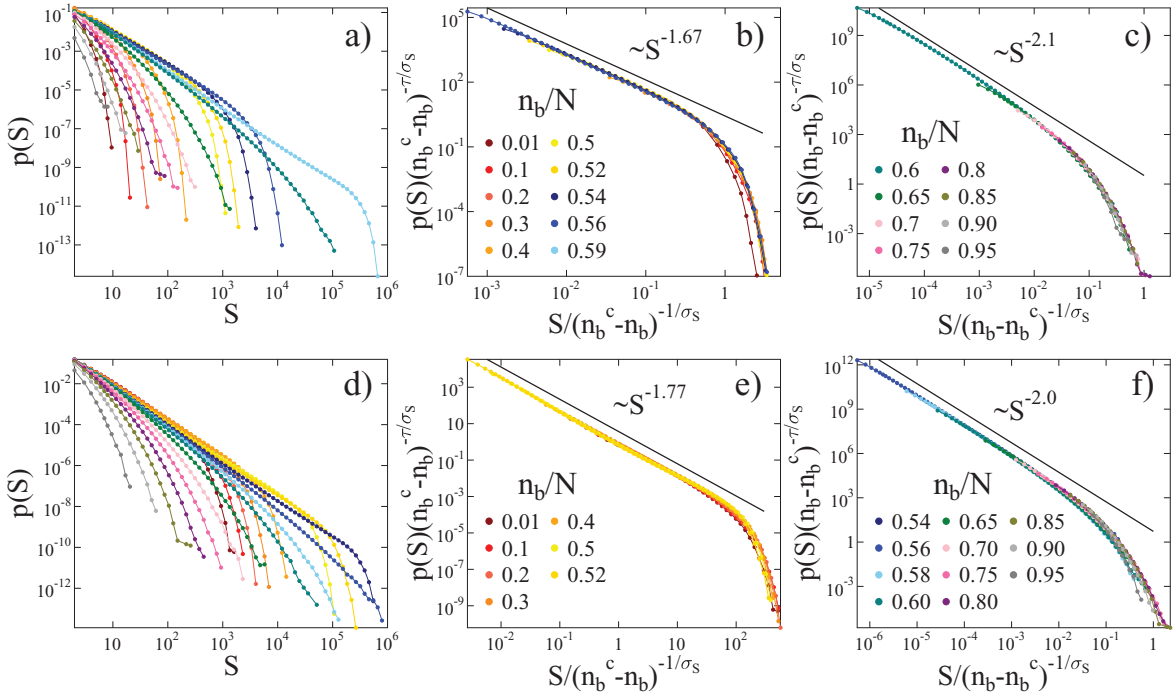

Figure 9. Size distribution of clusters $p(S)$ at several damage fractions n_b for $\mu = 0.1$ and $\mu = 0.9$ in the upper and lower rows respectively. In (a) and (d) distributions are presented covering the entire range of the damage fraction n_b. Data collapse of the curves is presented separately below (b), (e), and above (c), (f) the corresponding critical point n_b^c: $n_b^c = 0.598$ for $\mu = 0.1$ and $n_b^c = 0.548$ for $\mu = 0.9$. The legend used in (a) and (d) is the same as in $((b), (c))$ and $((e), (f))$ respectively.

of disorder is limited, i.e. when the disorder gets high fracture becomes unpredictable again. Heavy-tailed distributions of the failure thresholds of material elements give rise to a homogeneous fracture process which does not exhibit any sign of acceleration. Reducing the amount of disorder, the system undergoes a continuous phase transition to perfectly brittle failure, without restoring the ability of forecasting. In the mean field limit of the fiber bundle models (ELS) we determined analytically and numerically the critical exponents of the transition. On the macro-level the fracture strength of the bundle proved to increase with the system size—which is the direct consequence of the heavy-tailed distribution of fibers' strength defined over an infinite support. For practical purposes the case of a large but finite upper cutoff of local strength is also of high importance. Controlling the cutoff value a crossover is expected between the decreasing size dependence typical for moderate disorder FBMs and the increasing one revealed by the present study. The crossover is accompanied by the changing degree of stationarity of the time series of breaking bursts, which addresses an interesting question for failure forecast methods, as well.

In order to clarify how the inhomogeneous stress field developing around failed regions changes the evolution of the fracture process, we also studied the limit of localized load sharing where the load of a broken fiber is equally redistributed over its intact nearest neighbors. Even in this case fat tailed distributions proved to ensure the dominance of disorder over spatially correlated stress enhancements: the size distribution of

J. Stat. Mech. (2016) 073211

avalanches has a power law functional form with an exponent close to the mean field value. This is in strong contrast to what is usually found in LLS FBMs, i.e. a very rapidly decreasing distribution of avalanche sizes is usually obtained, which is described either by a power law of exponent 9/2 or by an exponential. Additionally, the continuous nature of the quasi-brittle to brittle transition remains in LLS, although the critical exponents have somewhat different values in the two limiting cases of load sharing. For LLS fiber bundles the spatial structure of damage strongly resembles the site percolation problem; deviations due to the presence of spatial correlations are obtained in the vicinity of the quasi-brittle to brittle phase transition. Although, for the lowest disorder $\mu \to 1$ the avalanche statistics and cluster structure of the LLS system shows the increasing role of spatial correlations, the macroscopic strength of the bundle is still consistent with the extreme order statistics obtained in ELS. The reason is that the time series of avalanches still exhibits a high degree of stationarity with the absence of a relevant acceleration and a catastrophic avalanche so that the strongest fibers can control macroscopic failure.

Based on our analytical and numerical results we conjecture that fat tailed strength distributions determine a unique universality class of the quasi-static fracture of fiber bundles. Recently, it has been demonstrated that 3D printing technology can be used to produce materials with finely tuned structural properties [31, 32]. In the near future it may also become possible to realize experimentally the limit of high disorder studied here.

Acknowledgments

We thank the projects TAMOP-4.2.2.A-11/1/KONV-2012-0036. This research was supported by the European Union and the State of Hungary, co-financed by the European Social Fund in the framework of TMOP-4.2.4.A/2-11/1-2012-0001 National Excellence Program.

References

[1] Herrmann H J and Roux S (ed) 1990 *Statistical Models for the Fracture of Disordered Media* (*Random Materials and Processes*) (Amsterdam: Elsevier)
[2] Alava M, Nukala P K and Zapperi S 2006 *Adv. Phys.* **55** 349–476
[3] Bazant Z P and Planas J 1997 *Fracture and Size Effect in Concrete and Other Quasibrittle Materials* (Boca Raton, FL: CRC Press)
[4] Alava M J, Nukala P K V V and Zapperi S 2009 *J. Phys. D: Appl. Phys.* **42** 214012
[5] Tárraga M, Carniel R, Ortiz R and García A 2008 Chapter 13: The failure forecast method: review and application for the real-time detection of precursory patterns at reawakening volcanoes *Caldera Volcanism: Analysis, Modelling and Response* (*Developments in Volcanology* vol 10) ed J Gottsmann and J Marti (Amsterdam: Elsevier) pp 447–69
[6] Bell A F, Greenhough J, Heap M J and Main I G 2011 *Geophys. J. Int.* **185** 718–23
[7] Dalmas D, Lelarge A and Vandembroucq D 2008 *Phys. Rev. Lett.* **101** 255501
[8] Ramos O, Cortet P P, Ciliberto S and Vanel L 2013 *Phys. Rev. Lett.* **110** 165506
[9] Vasseur J, Wadsworth F B, Lavallée Y, Bell A F, Main I G and Dingwell D B 2015 *Sci. Rep.* **5** 13259
[10] Roy S and Ray P 2015 *Europhys. Lett.* **112** 26004
[11] Halász Z, Danku Z and Kun F 2012 *Phys. Rev.* E **85** 016116
[12] Roy C, Kundu S and Manna S S 2015 *Phys. Rev.* E **91** 032103
[13] Raischel F, Kun F and Herrmann H J 2006 *Phys. Rev.* E **74** 035104
[14] Ciliberto S, Guarino A and Scorretti R 2001 *Physica* D **158** 83

J. Stat. Mech. (2016) 073211

[15] Manzato C, Alava M J and Zapperi S 2014 *Phys. Rev.* E **90** 012408
[16] Pradhan S, Hansen A and Chakrabarti B K 2010 *Rev. Mod. Phys.* **82** 499
[17] Kun F, Raischel F, Hidalgo R C and Herrmann H J 2006 Extensions of fiber bundle models *Modelling Critical and Catastrophic Phenomena in Geoscience: a Statistical Physics Approach* (*Lecture Notes in Physics*) ed P Bhattacharyya and B K Chakrabarti (Berlin: Springer) pp 57–92
[18] Galambos J 1978 *The Asymptotic Theory of Extreme Order Statistics* (New York: Wiley)
[19] Hansen A and Roux S 2000 Statistical toolbox for damage and fracture *Damage and Fracture of Disordered Materials* (*CISM Courses and Lectures* vol 410) ed D Krajcinovic and J V Mier (New York: Springer) pp 17–101
[20] Hidalgo R C, Kun F, Kovács K and Pagonabarraga I 2009 *Phys. Rev.* E **80** 051108
[21] Kloster M, Hansen A and Hemmer P C 1997 *Phys. Rev.* E **56** 2615–25
[22] Hemmer P C and Hansen A 1992 *J. Appl. Mech.* **59** 909–14
[23] Pradhan S, Hansen A and Hemmer P C 2006 *Phys. Rev.* E **74** 016122
[24] Pradhan S, Hansen A and Hemmer P C 2005 *Phys. Rev. Lett.* **95** 125501
[25] Danku Z, Kun F and Herrmann H J 2015 *Phys. Rev.* E **92** 062402
[26] Kovács K, Hidalgo R C, Pagonabarraga I and Kun F 2013 *Phys. Rev.* E **87** 042816
[27] Phoenix S L and Newman W I 2009 *Phys. Rev.* E **80** 066115
[28] Divakaran U and Dutta A 2007 *Int. J. Mod. Phys.* C **18** 6
[29] Kun F, Zapperi S and Herrmann H J 2000 *Eur. Phys. J.* B **17** 269
[30] Stauffer D and Aharony A 1992 *Introduction to Percolation Theory* (London: Taylor & Francis)
[31] Matsuzaki R, Ueda M, Namiki M, Jeong T K, Asahara H, Horiguchi K, Nakamura T, Todoroki A and Hirano Y 2016 *Sci. Rep.* **6** 23058
[32] Maiti A, Small W, Lewicki J P, Weisgraber T H, Duoss E B, Chinn S C, Pearson M A, Spadaccini C M, Maxwell R S and Wilson T S 2016 *Sci. Rep.* **6** 24871

J. Stat. Mech. (2016) 073211